

Article

Unprecedented Coordination Compounds with 4,4'-Diaminodiphenylethane as a Supramolecular Agent and Ditopic Ligand: Synthesis, Crystal Structures and Hirshfeld Surface Analysis

Nicoleta Craciun^{1,2}, Diana Chisca^{1,2}, Elena Melnic¹ and Marina S. Fonari^{1,*}¹ Institute of Applied Physics USM, Academiei Str. 5, MD-2028 Chisinau, Moldova² Faculty of Biology and Chemistry Ion Creangă State Pedagogical University, Ion Creangă Str. 1, MD-2069 Chisinau, Moldova

* Correspondence: marina.fonari@ifa.md or fonari.xray@gmail.com

Abstract: In this pioneering research, mononuclear coordination complexes and coordination polymers were obtained using the conformationally flexible ditopic ligand 4,4'-diaminodiphenylethane and different metal salts (nitrates, sulfates, tetrafluoroborates and perchlorates). Seven new products, including the mononuclear complexes $[\text{Cd}(2,2'\text{-bpy})_3](\text{ClO}_4)_2(\text{dadpe})(4,4'\text{-bpy})$ (**1**), $[\text{Ni}(\text{dadpe})_2(\text{H}_2\text{O})_4](\text{SO}_4)\cdot\text{H}_2\text{O}$ (**2**), one-dimensional coordination polymers $\{[\text{Zn}(\text{NO}_3)(\text{dadpe})(\text{dmf})_2](\text{NO}_3)\}_n$ (**3**), $\{[\text{Cd}(2,2'\text{-bpy})_2(\text{dadpe})](\text{ClO}_4)_2\}_n$ (**4**), and two-dimensional coordination polymers, $\{[\text{Cd}(4,4'\text{-bpy})_2(\text{H}_2\text{O})_2](\text{ClO}_4)_2(\text{dadpe})(\text{EtOH})_2\}_n$ (**5**), $\{[\text{Co}(4,4'\text{-bpy})_2(\text{H}_2\text{O})_2](\text{BF}_4)_2(\text{dadpe})(\text{EtOH})_2\}_n$ (**6**) and $\{[\text{Cd}(\text{adi})(\text{dadpe})](\text{H}_2\text{adi})\}_n$ (**7**), (dadpe=4,4'-diaminodiphenylethane, 2,2'-bpy=2,2'-bipyridine, 4,4'-bpy=4,4'-bipyridine, H₂adi=adipic acid) were produced. The synthesized compounds were characterized by FTIR and single-crystal X-ray diffraction analyses. The dadpe was recorded as a neutral guest in the crystals of mononuclear complex **1** and in coordination polymers **5** and **6**. In compound **2**, two dadpe ligands coordinate in a monodentate mode and occupy two trans-positions in the $[\text{Ni}(\text{H}_2\text{O})_4(\text{dadpe})_2]^{2+}$ octahedral complex cation. Coordination polymers **3** and **4** represent single chains originating from dadpe as a bidentate linker in both. The H-donor's possibilities of amino groups were utilized in the interconnection of coordination chains into H-bonded networks via $\text{NH}(\text{NH}_2)\cdots\text{O}$ hydrogen bonds. The isostructural coordination polymers **5** and **6** comprise similar cationic square grids $[\text{M}(4,4'\text{-bpy})_2(\text{H}_2\text{O})_2]^{2+}$ [M=Cd (**5**), M=Co (**6**)], with **sql** topology balanced by the charge-compensated anions, while dadpe and EtOH as neutral guests are situated in the interlayer space. The neutral 2D coordination network in **7** with the **sql** topology originates from both adi and dadpe linkers as bidentate-bridging ligands, and the neutral H₂adi is entrapped as a guest in crystal lattice. The impact of different types of intermolecular interactions was evaluated by Hirshfeld surface analysis.

Keywords: transition metals; synthesis; crystal structure; non-covalent interactions; Hirshfeld surface

Citation: Craciun, N.; Chisca, D.; Melnic, E.; Fonari, M.S. Unprecedented Coordination Compounds with 4,4'-Diaminodiphenylethane as a Supramolecular Agent and Ditopic Ligand: Synthesis, Crystal Structures and Hirshfeld Surface Analysis. *Crystals* **2023**, *13*, 289. <https://doi.org/10.3390/cryst13020289>

Academic Editor: Waldemar Maniukiewicz

Received: 24 January 2023

Revised: 3 February 2023

Accepted: 5 February 2023

Published: 8 February 2023



Copyright: © 2023 by the authors. Licensee MDPI, Basel, Switzerland. This article is an open access article distributed under the terms and conditions of the Creative Commons Attribution (CC BY) license (<https://creativecommons.org/licenses/by/4.0/>).

1. Introduction

For decades, 4,4'-bipyridine (4,4'-bpy), its longer homologues and modified derivatives were widely used as bidentate-bridging ligands in the synthesis of coordination polymers, giving rise either to cationic polymeric arrays when combined with easy-leaving anions [1–4], or to neutral coordination networks when used in a partnership with strongly coordinated anions such as polycarboxylates [5–8]. Although ditopic amino-ligands are weaker bases than the five- and six-membered heterocyclic N-bases, the presence of terminal amino groups gives them the advantage of simultaneous coordination with the metal and participation in different hydrogen bonds and weak interactions reinforcing the crystal lattice [9–11]. Moreover, the NH₂-group in organic luminescent materials is

regarded as an electron-donating group suitable for binding the electron-accepting metal ions. Compounds containing such amino ligands show luminescence through intraligand p–p* transitions [12].

So far, a significant number of coordination compounds, including silver and cadmium coordination polymers, were documented [13] for 4,4'-diaminodiphenylmethane [10–12,14]. Silver and cadmium coordination polymers were also obtained with the more extended ditopic ligand, 4,4'-(1,4-phenylenediisopropylidene)bis(aniline) [15,16]. The 3,3'-diaminobiphenylsulfone was reported to trap heavy metals (Cu(II), Hg(II)) in the form of coordination compounds [17,18]. On the other hand, no coordination compounds with 4,4'-diaminodiphenylmethane (dadpe, also known under the names 4,4'-diaminobibenzyl, 4,4'-ethylenedianiline), the closest homologue of 4,4'-diaminodiphenylmethane, were yet reported. The survey of CSD (Version 5.43, November 2022 updates) only disclosed the dadpe in the form of hydrate [19], and as a guest in the inclusion compound with beta-cyclodextrin (β -CD) [20]. In the crystal of the hydrate, a dadpe molecule was registered in an extended trans-conformation. Alternatively, the same molecule exhibited one extended and two bent conformations in the inclusion complex with β -CD [20]. The expected and registered conformational flexibility of dadpe was an additional benefit for its use in the synthesis of flexible coordination networks. The flexible CPs reveal some advantages and attractive applications compared with the rigid frameworks. For example, they show pore opening and significantly increased adsorption capacity [21]. In this pioneering work, we report the synthesis, IR spectroscopic characterization and crystal structures for seven coordination compounds obtained from the different metal salts, $\text{Cd}(\text{ClO}_4)_2 \cdot 2\text{H}_2\text{O}$, $\text{Cd}(\text{NO}_3)_2 \cdot 4\text{H}_2\text{O}$, $\text{NiSO}_4 \cdot 7\text{H}_2\text{O}$, $\text{Co}(\text{BF}_4)_2 \cdot 6\text{H}_2\text{O}$, $\text{Zn}(\text{NO}_3)_2 \cdot 6\text{H}_2\text{O}$ and a ditopic dadpe ligand. New coordination compounds include mononuclear complexes $[\text{Cd}(2,2'\text{-bpy})_3](\text{ClO}_4)_2(\text{dadpe})(4,4'\text{-bpy})$ (1), $[\text{Ni}(\text{dadpe})_2(\text{H}_2\text{O})_4](\text{SO}_4) \cdot 2\text{H}_2\text{O}$ (2), one-dimensional (1D) coordination polymers $\{[\text{Zn}(\text{NO}_3)(\text{dadpe})(\text{dmf})_2](\text{NO}_3)\}_n$ (3), $\{[\text{Cd}(2,2'\text{-bpy})_2(\text{dadpe})](\text{ClO}_4)_2\}_n$ (4), and two-dimensional (2D) coordination polymers, $\{[\text{Cd}(4,4'\text{-bpy})_2(\text{H}_2\text{O})_2](\text{ClO}_4)_2(\text{dadpe})(\text{EtOH})_2\}_n$ (5), $\{[\text{Co}(4,4'\text{-bpy})_2(\text{H}_2\text{O})_2](\text{BF}_4)_2(\text{dadpe})(\text{EtOH})_2\}_n$ (6) and $\{[\text{Cd}(\text{adi})(\text{dadpe})](\text{H}_2\text{adi})\}_n$ (7). The distribution of intermolecular interactions in compounds 1, 2, 3 and 7, which reveal different structural functions of dadpe ligand (as a neutral guest, a monodentate terminal ligand, and a bidentate-bridging ligand), was evaluated by Hirshfeld surface analysis.

2. Materials and Methods

2.1. Materials and Measurements

The starting salts, organic ligands and solvents were obtained from commercial sources (Sigma-Aldrich, St. Louis, MO, USA) and were used without further purification. The IR(ATR) spectra were recorded on a FTIR Spectrum-100 Perkin Elmer spectrometer in the range of 4000–650 cm^{-1} . Elemental analysis was performed on a Vario EL III Element Analyzer.

2.2. Synthesis

2.2.1. $[\text{Cd}(2,2'\text{-bpy})_3](\text{ClO}_4)_2(\text{dadpe})(4,4'\text{-bpy})$ (1)

Compound 1 was prepared with the hydrothermal method. Dadpe 0.04 g (0.2 mmol) was dissolved in 7 mL EtOH. In this solution, 0.03 g (0.1 mmol) $\text{Cd}(\text{ClO}_4)_2 \cdot 2\text{H}_2\text{O}$, 0.045 g (0.3 mmol) 2,2'-bpy and 0.045 g (0.3 mmol) 4,4'-bpy, were added successfully. The obtained solution was placed in a 20 mL Teflon-lined stainless steel autoclave, which was then sealed and heated to 100 °C for 20 h. The solution was filtered and left for slow evaporation at room temperature. After 72 h, colorless crystals were filtered and dried in the air (yield 57%). Anal. Calc. for $\text{C}_{42}\text{H}_{36}\text{CdCl}_2\text{N}_8\text{O}_8$ (%): C, 52.32; H, 3.76; N, 11.62. Found: C, 52.98; H, 3.49; N, 11.04. IR-ATR (cm^{-1}): 3439 m, 3355 m, 1611 m, 1515 s, 14,382, 1278 m, 1193 w, 1083 s, 1024 m, 970 w, 819 s, 762 s, 735 w, 648 w, 621 m, 527 s, 488 w, 411 m.

2.2.2. $[\text{Ni}(\text{dadpe})_2(\text{H}_2\text{O})_4](\text{SO}_4) \cdot \text{H}_2\text{O}$ (2)

Dadpe 0.02 g (0.1 mmol) was dissolved in 5 mL EtOH. After that, 0.02 g (0.1 mmol) of $\text{NiSO}_4 \cdot 7\text{H}_2\text{O}$ was added. The reaction mixture was refluxed with stirring for 20 min

at 80 °C. A white precipitate formed and was dissolved with 3 mL of H₂O_{dist}. The solution was filtered and left for slow evaporation at room temperature. After 7 days, the crystals of yellow color were filtered, and dried in the air (yield ~60%). Anal. Calc. for C₂₈H₄₄N₄NiO₁₀S (%): C, 48.92; H, 6.45; N, 8.15. Found: C, 48.38; H, 5.99; N, 8.24. IR-ATR (cm⁻¹): 3392 m, 3310 m, 2976 w, 2917 w, 2854 w, 1614 s, 1514 s, 1455 w, 1281 m, 1250 m, 1173 s/h, 1057 s, 939 w, 833 s, 537 s.

2.2.3. {[Zn(NO₃)(dadpe)(dmf)₂](NO₃)_n} (3)

Dadpe 0.02 g (0.1 mmol) was dissolved in 10 mL mixture CH₃CN:EtOH (5:5). In this solution, 0.018 g (0.1 mmol) Zn(NO₃)₂·6H₂O and 3 mL DMF were added. The mixture was positioned in an ultrasonic bath, at ambient temperature and atmospheric pressure for 30 min. The solution was filtered and left for slow evaporation at room temperature. After 150 days, light-yellow crystals were filtered, and dried in the air (yield ~47%). Anal. Calc. for C₂₀H₃₀N₆O₈Zn (%): C, 43.85; H, 5.52; N, 15.34. Found: C, 43.35; H, 5.19; N, 14.99. IR-ATR (cm⁻¹): 3440 m, 3376 m, 3355 m, 3300 m, 3230 m, 3146 m, 3011 m, 2915 m, 2852 m, 2360 s, 2343 s, 1617 s, 1515 s, 1475 w, 1437 m, 1363 m, 1313 s, 1280 s, 1250 m, 1170 w, 1113 s, 1084 s, 1015 s, 947 w, 913 w, 820 s, 762 m, 735 m, 669 m, 621 m, 527 s, 408 m.

2.2.4. {[Cd(2,2'-bpy)₂(dadpe)](ClO₄)₂]_n} (4)

To a cold solution of dadpe 0.04 g (0.2 mmol) in 7 mL EtOH, Cd(ClO₄)₂·2H₂O 0.03 g (0.1 mmol) and 2,2'-bpy 0.05 g (0.3 mmol) were added and continuously stirred. The obtained solution was placed in a 20 mL Teflon-lined stainless steel autoclave which was then sealed and heated to 80 °C for 17 h. The solution was filtered and left for slow evaporation at room temperature. After 24 h, crystals of a light green color were filtered and dried in the air (yield ~58%). Anal. Calc. for C₃₄H₃₂CdCl₂N₆O₈ (%): C, 48.85; H, 3.86; N, 10.05. Found: C, 48.95; H, 2.99; N, 10.25. IR-ATR (cm⁻¹): 3320 m, 3258 m, 1595 m, 1515 m, 1438 s, 1318 m, 1246 w, 1226 m, 1083 s, 1013 s, 936 m, 823 m, 756 s, 736 n, 618 s, 521 m, 478 w.

2.2.5. {[Cd(4,4'-bpy)₂(H₂O)₂](ClO₄)₂(dadpe)(EtOH)₂]_n} (5)

To a cold solution of dadpe 0.04 g (0.2 mmol) in 7 mL EtOH, Cd(ClO₄)₂·2H₂O 0.04 g (0.2 mmol) and 4,4'-bpy 0.03 g (0.1 mmol) were added. The reaction mixture was refluxed with stirring for 20 min at 80 °C. The solution was filtered and left for slow evaporation at room temperature. After 6 days, light brown crystals were filtered and dried in the air (yield ~63%). Anal. Calc. for C₃₈H₄₈CdCl₂N₆O₁₂ (%): C, 47.34; H, 5.02; N, 8.72. Found: C, 47.94; H, 4.99; N, 8.94. IR-ATR (cm⁻¹): 3440 m, 3355 m, 3113 w, 3069 w, 1595 s, 1518 s, 1477 s, 1437 s, 1321 m, 1280 m, 1249 s, 1177 w, 1163 w, 1076 s, 1013 s, 977 m, 840 m, 762 s, 762 m, 68 m, 619 s, 528 m.

2.2.6. {[Co(4,4'-bpy)₂(H₂O)₂](BF₄)₂(dadpe)(EtOH)₂]_n} (6)

Dadpe 0.04 g (0.2 mmol) was dissolved in 7 mL EtOH. To this solution, 0.034 g (0.1 mmol) Co(BF₄)₂·6H₂O and 0.03 g (0.2 mmol) 4,4'-bpy were added successfully. The obtained solution was placed in a 20 mL Teflon-lined stainless steel autoclave which was then sealed and heated to 100 °C for 20 h. The solution was filtered off and left for slow evaporation at a room temperature. After 24 h, light brown crystals were filtered off and dried in the air (yield ~46%). Anal. Calc. for C₃₈H₄₈B₂CoF₈N₆O₄ (%): C, 51.55; H, 5.46; N, 9.49. Found: C, 51.99; H, 5.09; N, 8.99. IR-ATR (cm⁻¹): 3553 m, 3480 m, 3359 m, 1605 s, 1535 m, 1515 s, 1490 m, 1411 s, 1394 s/h, 1301 w, 1221 s, 1173 w, 1064 s, 1049 s, 1003 s, 972 s/h, 883 m, 850 m, 809 s, 732 m, 681 w, 628 s, 585 m, 541 m, 519 m, 469 m.

2.2.7. {[Cd(adi)(dadpe)](H₂adi)]_n} (7)

In a first beaker, 0.02 g (0.1 mmol) of dadpe was dissolved in 3 mL MeOH. In another beaker, 0.03 g (0.1 mmol) of Cd(NO₃)₂·4H₂O and 0.01 g (0.1 mmol) of H₂adi were dissolved in 5 mL EtOH. The solutions were mixed upon stirring. To the white precipitate, 5 mL

H₂O_{dist.} was added. The mixture was positioned in an ultrasonic bath at ambient temperature and atmospheric pressure for 30 min. The solution was filtered off and left for slow evaporation at a room temperature. After 30 days, light yellow crystals were filtered off and dried in the air (yield ~61%). Anal. Calc. for C₂₆H₃₄CdN₂O₈ (%): C, 50.78; H, 5.57; N, 4.56. Found: C, 51.06; H, 5.89; N, 4.99. IR-ATR (cm⁻¹): 3239 m, 3151 m, 2925 m, 1694 s, 1617 m, 1512 s, 1455 m, 1408 s, 1331 m, 1263 m, 1229 s, 1183 m, 1136 s, 1060 s, 820 s, 656 s, 542 s, 452 s.

2.3. Single Crystal X-ray Analysis

Single crystal X-ray diffraction measurements for **1–7** were carried out on an Xcalibur E diffractometer equipped with a CCD area detector and a graphite monochromator, utilizing MoK α radiation at a room temperature. Final unit cell dimensions were obtained and refined on entire datasets. All calculations to solve the structures and to refine the models proposed were carried out with the programs SHELXS97 and SHELXL2014 [22,23]. The disordering problems were resolved for weakly bound perchlorate anion in **1**, **4**, **5**, tetrafluoroborate anion in **6**, dadpe ligand in **4**, and EtOH solvent molecule in **5** and **6**. Whenever necessary, restraints were imposed on the geometry and displacement parameters of disordered molecules. C-bound H-atoms were positioned geometrically and treated as riding atoms using SHELXL default parameters with $U_{\text{iso}}(\text{H}) = 1.2U_{\text{eq}}(\text{C})$ and $U_{\text{iso}}(\text{H}) = 1.5U_{\text{eq}}(\text{CH}_3)$. N(O)-bound H-atoms were found predominantly from the difference Fourier maps and refined at the final stages using geometric constraints to keep the geometry of amino groups and water molecules reliable. The X-ray data and details of the refinement for **1–7** are summarized in Table 1. The principal bond distances and angles in **1–7** have common values and are summarized in Table S1. The geometric parameters of H-bonds are given in Table S2 (see Supporting Information file). The figures were produced using MERCURY [24]. The solvent-accessible areas were evaluated using MERCURY [24] and PLATON [25] facilities. CIF files for **1–7** that contain all crystallographic details may be obtained free of charge from the Cambridge Crystallographic Data Centre (<https://www.ccdc.cam.ac.uk/structures/>, accessed on 16 January 2023) by quoting the CCDC deposition numbers 2236422–2236428.

Table 1. Crystal data and structure refinement parameters for 1–7.

	1	2	3	4	5	6	7
CCDC deposition number	2236422	2236423	2236424	2236425	2236426	2236427	2236428
Empirical formula	C ₄₂ H ₃₆ CdCl ₂ N ₈ O ₈	C ₂₈ H ₄₄ N ₄ NiO ₁₀ S	C ₂₀ H ₃₀ N ₆ O ₈ Zn	C ₃₄ H ₃₂ CdCl ₂ N ₆ O ₈	C ₃₈ H ₄₈ CdCl ₂ N ₆ O ₁₂	C ₃₈ H ₄₈ B ₂ CoF ₈ N ₆ O ₄	C ₂₆ H ₃₄ CdN ₂ O ₈
<i>T</i> , K	293(2)	293(2)	293(2)	293(2)	293(2)	293(2)	293(2)
<i>FW</i> (g mol ^{−1})	964.09	687.44	547.87	835.95	964.12	885.37	614.95
Crystal system	Triclinic	Monoclinic	Orthorhombic	Monoclinic	Monoclinic	Monoclinic	Monoclinic
Space group	<i>P</i> -1	<i>P</i> ₂ ₁ / <i>c</i>	<i>Pbca</i>	<i>P</i> ₂ ₁ / <i>c</i>	<i>C</i> ₂ / <i>c</i>	<i>C</i> ₂ / <i>c</i>	<i>P</i> ₂ / <i>c</i>
<i>a</i> /Å	11.4066(6)	18.195(2)	17.2741(10)	10.5752(5)	19.5958(5)	19.0858(14)	13.0429(4)
<i>b</i> /Å	13.2070(6)	10.053(2)	10.4778(4)	13.6755(6)	11.7421(2)	11.4429(4)	5.1903(2)
<i>c</i> /Å	14.1328(8)	9.1989(7)	28.0153(11)	24.4455(19)	20.1263(6)	22.5537(18)	19.9688(6)
<i>α</i> /deg	96.087(4)	90	90	90	90	90	90
<i>β</i> /deg	104.337(5)	101.660(7)	90	91.488(5)	108.939(3)	121.947(11)	100.079(3)
<i>γ</i> /deg	96.049(4)	90	90	90	90	90	90
<i>V</i> /Å ³	2031.89(19)	1648.0(3)	5070.6(4)	3534.1(4)	4380.3(2)	4179.6(6)	1330.96(8)
<i>Z</i>	2	2	8	4	4	4	2
<i>D</i> _{calcd} Mg/m ³	1.576	1.385	1.435	1.571	1.462	1.407	1.534
<i>μ</i> /mm ^{−1}	0.734	0.711	1.023	0.829	0.686	0.493	0.871
<i>F</i> (000)	980	728	2288	1696	1984	1836	632
Reflections collected	11770	5343	12232	13628	7798	7782	4527
Independent reflections	7176 [<i>R</i> (int) = 0.0303]	2906 [<i>R</i> (int) = 0.0242]	4692 [<i>R</i> (int) = 0.0615]	6523 [<i>R</i> (int) = 0.0471]	4070 [<i>R</i> (int) = 0.0204]	4083 [<i>R</i> (int) = 0.0293]	2620 [<i>R</i> (int) = 0.0200]
Data/restraints/parameters	7176/92/572	2906/22/239	4692/19/320	6523/82/524	4070/169/341	4083/114/339	2620/15/193
GOF	1.001	1.000	1.000	1.005	1.092	0.999	1.004
<i>R</i> indices [<i>I</i> > 2σ(<i>I</i>)], <i>R</i> ₁ , <i>wR</i> ₂	0.0464, 0.1036	0.0498, 0.1413	0.0559, 0.0797	0.0600, 0.1230	0.0373, 0.0916	0.0525, 0.1419	0.0293, 0.0720
<i>R</i> indices (all data), <i>R</i> ₁ , <i>wR</i> ₂	0.0630, 0.1139	0.0711, 0.1573	0.1162, 0.0938	0.1301, 0.1524	0.0441, 0.0949	0.0734, 0.1545	0.0336, 0.0749

3. Results and Discussion

3.1. FTIR Characterization of 1–7

The FTIR spectra for compounds 1–7 confirm the presence of the ligands used in the syntheses (Figure 1 and Figures S1–S7 in the Supporting Information file). The occurrence of the dadpe ligand is indicated by stretching vibrations of amino groups registered in two spectral ranges: at high frequencies, 3440–3330 cm^{-1} characteristic for hydrogen stretching, and in the range 1277–1250 cm^{-1} which is typical for asymmetric and symmetric stretching vibrations of C-N bond of aromatic amines [19]. This shows great similarity with the aniline stretching C-N mode at 1276 cm^{-1} [26]. At high frequencies, the broad IR bands attributed to the stretching O-H vibrations of coordinated water molecules in 2, 5, 6 were also registered. The asymmetric and symmetric methylene C-H stretching vibrations come out as 2976 and 2854 cm^{-1} bands in 2, and a 2852 cm^{-1} band in 3 in the IR spectra. The stretching vibration of the central C-C bond is mainly localized at 1083–1003 cm^{-1} . Four types of bending modes (scissoring, twisting, wagging, and rocking) are inherent for the terminal $-\text{NH}_2$ and central $-\text{CH}_2-$ groups of ethane fragment, but they occur with weak intensities, and for NH_2 -group were registered at 1515, and 850–735 cm^{-1} , respectively. It is worth noting that all of these modes are strongly mixed with vibrations of phenyl and pyridyl rings, and the rings' predominantly stretching vibrations are assigned to the range of 1650–1400 cm^{-1} , while the rings' predominantly bending vibrations are assigned to the range of 1400 to 400 cm^{-1} . In 7, the characteristic asymmetric stretching vibrations of the carboxylic group appear at 1617 cm^{-1} , and the bands in the range of 1450 to 1308 cm^{-1} are attributed to the symmetric stretching mode of carboxylic groups. The strong IR band at 1694 cm^{-1} also indicates the presence of neutral H_2adi in the crystal structure. The IR bands in the region of 1310 to 1000 cm^{-1} are attributed to the $-\text{CH}-$ in-plane or out-of-plane bending modes, ring breathing, and ring deformation frequencies of the pyridine ring, respectively.

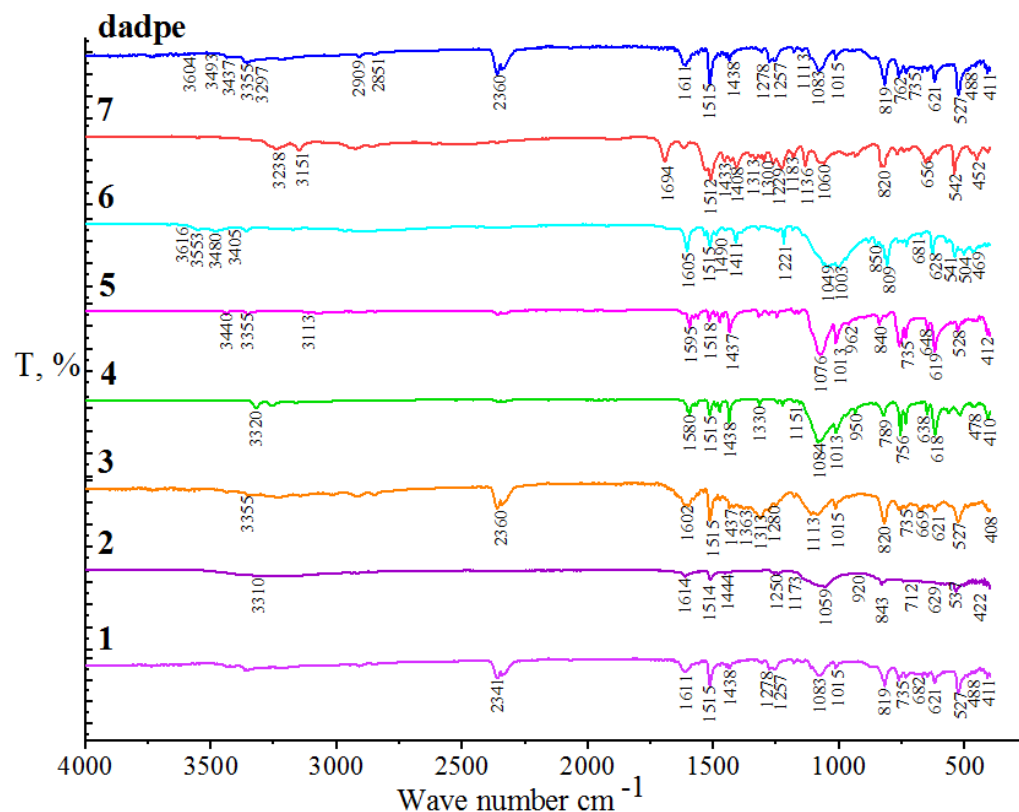


Figure 1. Combined diagram of IR spectra for 1–7 and dadpe ligand.

3.2. X-ray Study

3.2.1. Mononuclear Complexes

Competition of 2,2'-bpy and 4,4'-bpy with dadpe as a weaker N-base resulted in mononuclear complex $[\text{Cd}(2,2'\text{-bpy})_3](\text{ClO}_4)_2(\text{dadpe})(4,4'\text{-bpy})$ (**1**). The asymmetric part of the triclinic unit cell comprises one complex cation $[\text{Cd}(2,2'\text{-bpy})_3]^{2+}$, one non-bound charge-compensated ClO_4^- anion and halves of centrosymmetric 4,4'-bpy and dadpe molecules as the guests (Figure 2a). A Cd atom is situated in general position, and its N_6 -octahedral coordination geometry forms three 2,2'-bpy ligands coordinated in bidentate-chelate coordination modes with Cd-N distances varying in the narrow range, 2.324(3)–2.379(3) Å. Geometry of the complex cation is consistent with the reported examples [27,28]. In the crystal, stacking interactions prevail, since each blade of the three-blade propeller-type $[\text{Cd}(2,2'\text{-bpy})_3]^{2+}$ cation participates in its own stacking pattern, being centrosymmetric dimer 2,2'-bpy/2,2'-bpy with an interplanar separation of 3.491 Å, and two stacking trimers, namely 2,2'-bpy/4,4'-bpy/2,2'-bpy (with 4,4'-bpy situated at equidistant distances, 3.47–3.49 Å between two 2,2'-bpy), and 2,2'-bpy/dadpe/2,2'-bpy (with 2,2'-bpy-2,2'-bpy separation of 7.427 Å, Figure 2b). The centrosymmetric dadpe molecule takes an extended conformation with phenyl rings situated in parallel planes and a -C-CH₂-CH₂-C- torsion of 180.0°. No meaningful hydrogen bonds with participation of dadpe amino groups were registered in this structure; alternatively, the outer-sphere ClO_4^- anion was involved only in weak $\text{CH}\cdots\text{O}$ interactions (Table S2).

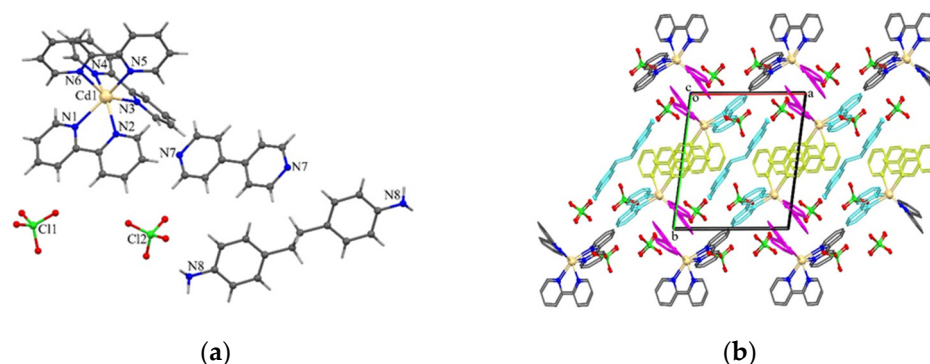


Figure 2. Compound **1**. (a) View of components in **1** with partial labelling scheme. (b) Fragment of crystal packing with stacking patterns colored magenta for 2,2'-bpy/2,2'-bpy dimer; yellow for 2,2'-bpy/4,4'-bpy/2,2'-bpy trimer; and cyan for 2,2'-bpy/dadpe/2,2'-bpy trimer.

Mononuclear complex $[\text{Ni}(\text{dadpe})_2(\text{H}_2\text{O})_4](\text{SO}_4)\cdot 2\text{H}_2\text{O}$ (**2**) comprises an octahedral complex cation $[\text{Ni}(\text{H}_2\text{O})_4(\text{dadpe})_2]^{2+}$, an outer-sphere charge-balanced sulfate anion and a solvent water molecule (Figure 3a). A Ni atom, lying on an inversion center, is bound with two dadpe ligands [Ni–N 2.143(3) Å] situated in trans-positions and four water molecules [Ni–O 2.046(2) Å]. Two identical monodentate dadpe ligands have extended conformations with -C-CH₂-CH₂-C- torsion of 178.3(4)°, and provide the longitude of the complex cation of 27.121(6) Å. Components in the crystal are linked in the 3D H-bonded network via a plethora of hydrogen bonds, with participation of both coordinated and non-coordinated amino groups (Figure 3b, Table S2).

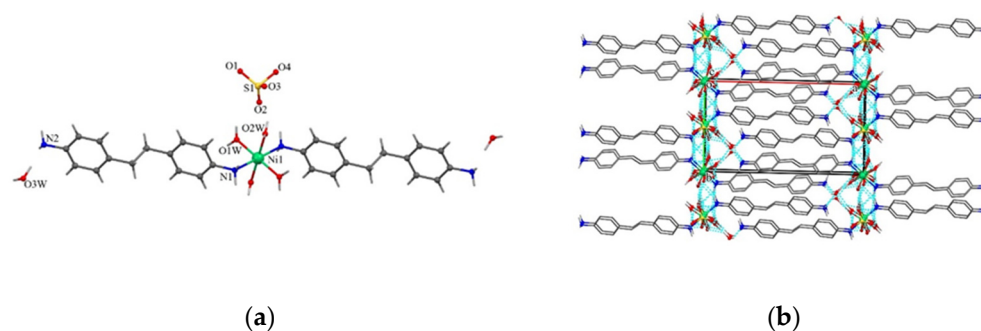


Figure 3. Compound 2. (a) View of complex 2 with partial labelling scheme. (b) Crystal packing with indication of principal hydrogen bonds.

3.2.2. 1D Coordination Polymers

Compound $\{[\text{Zn}(\text{NO}_3)(\text{dadpe})(\text{dmf})_2](\text{NO}_3)\}_n$ (**3**) comprises a linear positively charged coordination polymeric chain $[\text{Zn}(\text{NO}_3)(\text{dadpe})(\text{dmf})_2]_n^+$ running along the coordination *c* axis and one outer sphere charge-compensated nitrate anion. The dadpe takes a slightly twisted extended trans-conformation, with a $-\text{C}-\text{CH}_2-\text{CH}_2-\text{C}-$ torsion of $177.3(4)^\circ$ and an interplanar Ph/Ph angle of 6.36° , and provides Zn \cdots Zn separation of $14.041(8) \text{ \AA}$ along the coordination chain. The Zn atom is situated in general position and takes a distorted N_2O_4 octahedral coordination geometry originating from one nitrate anion that coordinates in a bidentate-chelate mode, two monodentate trans-situated dmf molecules and two bidentate-bridging dadpe ligands situated in neighboring positions [the bond angle $\text{N}(5^*)-\text{Zn}(1)-\text{N}(4) = 106.62(12)^\circ$, Table S1] and each facing the O-atom of the chelate nitrate-group (Figure 4a). The rather similar coordination environment for Zn(II) was registered in 4,13-bis(2-aminobenzyl)-4,13-diaza-18-crown-6-bis(nitrato-*O,O'*)-zinc(II) where two nitrate anions are fixed similarly at long Zn-O(NO_3) distances, 2.336 and 2.370 \AA [29]. The proximal arrangement of dadpe ligands in **3** is reinforced by their involvement in two $\text{NH}(\text{NH}_2) \cdots \text{O}(\text{NO}_3)$ hydrogen bonds (Table S2), with an outer-sphere nitrate anion situated in a perching position and reproaching these ligands (Figure 4a). The cationic chains situated parallel with the *c* axis are interconnected along the *b*-axis by $\text{NH}(\text{NH}_2) \cdots \text{O}(\text{NO}_3)$ hydrogen bonds from the same O-atoms of the outer sphere nitrate anion again (Table S2), thus combining the coordination chains in the H-bonded thick layer situated parallel to the *bc* plane (Figure 4b). All the meaningful hydrogen bonds, with the participation of two NH_2 -groups, are realized within this H-bonded thick layer restricted by the coordinated nitrate anions (Figure 4c).

Similar to compound **3**, compound $\{[\text{Cd}(2,2'\text{-bpy})_2(\text{dadpe})](\text{ClO}_4)_2\}_n$ (**4**) crystallizes as a linear positively charged polymeric coordination chain $\{[\text{Cd}(2,2'\text{-bpy})_2(\text{dadpe})]_n^{2+}$ (Figure 5a), but with both ClO_4^- as outer sphere counter-ions. A Cd(II) atom takes a distorted octahedral N_6 coordination geometry originating from two bidentate-chelate 2,2'-bpy ligands and two bidentate-bridging dadpe ligands that are situated in neighboring cis-positions, angle $\text{N}(\text{NH}_2)-\text{Cd}-\text{N}(\text{NH}_2) = 95.9(2)^\circ$, with Cd-N bonds ranging $2.345(5)$ – $2.371(5) \text{ \AA}$. The dadpe linker has a twisted conformation with an interplanar angle of 73.44° between the phenyl rings, affording Cd \cdots Cd separation of $13.6755(8) \text{ \AA}$ along the coordination chain running parallel to the *b* axis. Such a twisted conformation of dadpe makes it possible for the intrachain 2,2'-bpy/Ph to partially overlap with the proximity of the Cd atom. In this structure, in a mode similar to **3**, one of two crystallographically unique ClO_4^- anions chelates the neighboring NH_2 -groups via a couple of $\text{NH}(\text{NH}_2) \cdots \text{O}(\text{ClO}_4^-)$ H-bonds, while the second ClO_4^- anion mediates the neighboring chains along the crystallographic *a* axis via two other H-atoms of each amino group, thus combining the coordination chains in porous H-bonded layer parallel to the AB plane (Figure 5b). Similar to **3**, amino groups of bidentate-bridging coordinated dadpe ligands are completely involved in the H-bonds in the crystal. The neighboring coordination chains meet in the crystal by the 2,2'-bpy edges without overlap (Figure 5c).

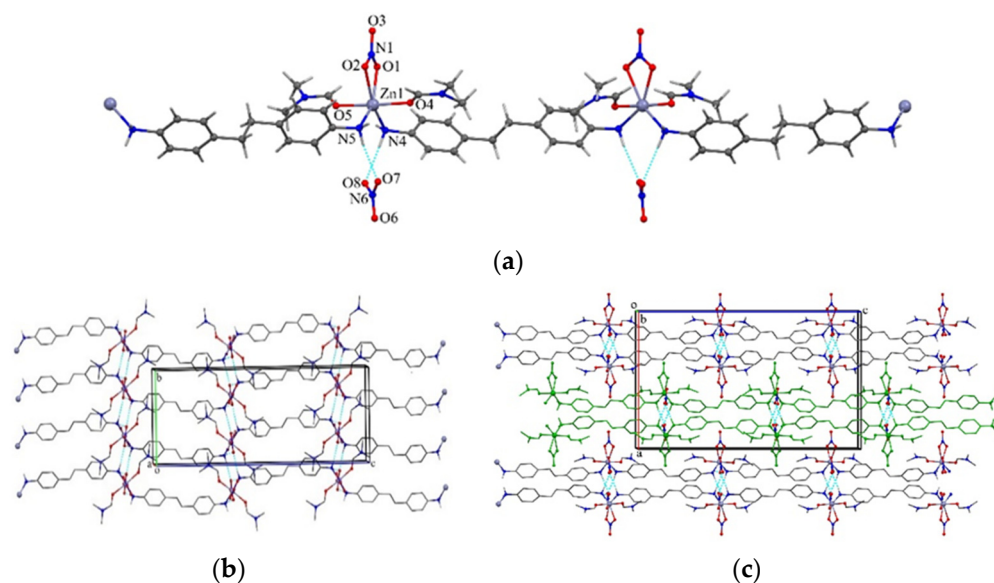


Figure 4. Compound 3. (a) Fragment of cationic polymeric chain with outer sphere nitrate anions attached by H-bonds. (b) Association of coordination chains in the H-bonded layer, view along the *a*-axis; (c) Stacking of the H-bonded layers in the crystal in the ABA manner along the *a* axis.

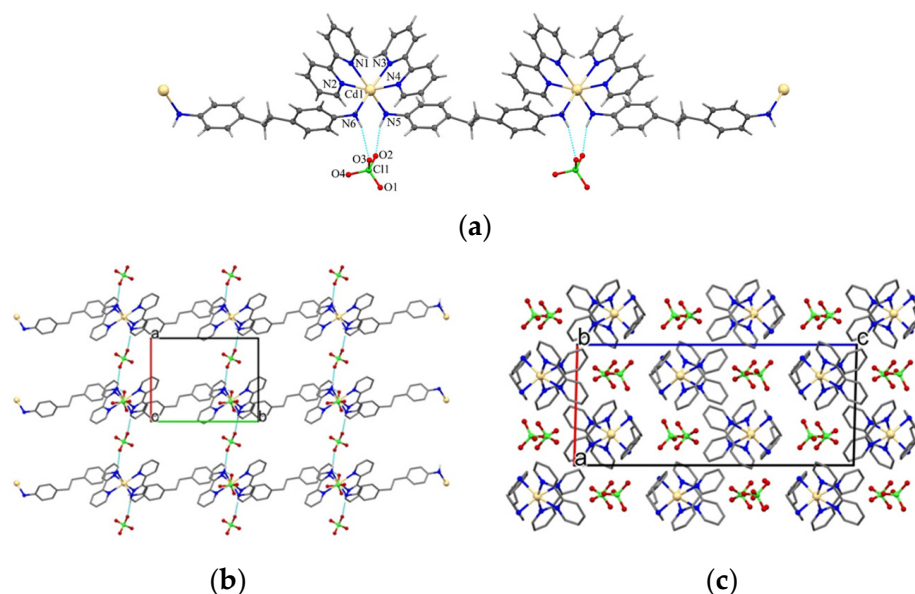


Figure 5. Compound 4. (a) Fragment of cationic polymeric chain with outer-sphere perchlorate-anions attached by H-bonds. (b) Association of coordination chains in the H-bonded layer, view along the *b*-axis; (c) Crystal packing.

3.2.3. 2D Coordination Polymers

Two isostructural compounds $\{[\text{Cd}(4,4'\text{-bpy})_2(\text{H}_2\text{O})_2](\text{ClO}_4)_2(\text{dadpe})(\text{EtOH})_2\}_n$ (**5**) and $\{[\text{Co}(4,4'\text{-bpy})_2(\text{H}_2\text{O})_2](\text{BF}_4)_2(\text{dadpe})(\text{EtOH})_2\}_n$ (**6**) crystallize in the monoclinic $C2/c$ space group (Table 1) and comprise the positively charged square grid frameworks $[\text{M}(4,4'\text{-bpy})_2(\text{H}_2\text{O})_2]^{2+}$ [$\text{M}=\text{Cd}$ (**5**), $\text{M}=\text{Co}$ (**6**)] with **sql** topology, outer-sphere charge-compensated anions $[\text{ClO}_4^-$ (**5**), BF_4^- (**6**)], and the neutral guests, dadpe and EtOH (Figure 6a). Two coordinated 4,4'-bpy ligands obey C_1 and C_2 point group symmetries and have planar and twisted geometries. The rectangular meshes in the cationic grids have linear dimensions of $11.742 \times 11.786 \text{ \AA}^2$ in **5** and $11.443 \times 11.514 \text{ \AA}^2$ in **6**. The inspection of CSD [13] revealed only few examples with the same 2D grids exclusively for Cu(II) as a central metal [1,30,31]. In those seminal works, the fascinating properties of such networks were registered as

dynamic anion exchange, possibility to accommodate tremendous aggregates such as polyoxometalates (POMs) in the voids of 2D networks. The reported polymers **5** and **6** also demonstrated the possibility of impressive loading of these crystals through incorporation of framework-regulated anions and bulky neutral molecules; dadpe and EtOH solvent were held in the interlayer space via an extensive H-bonding network including neutral and anionic guest species and water molecules of coordinated scaffold (Table S2). Similar to compound **1**, in compounds **5** and **6**, the dadpe guest molecules reside on inversion centers and take an ideal trans-conformation. The meaningful solvent accessible volumes (SAV) comprise 2151.7 Å³ (49.1%) of 4380.3 Å³ unit cell volume in **5** and 2063.2 Å³ (49.4%) of 4179.6 Å³ unit cell volume in **6**, as calculated by PLATON after evacuation of dadpe and EtOH molecules (Figure 6b).

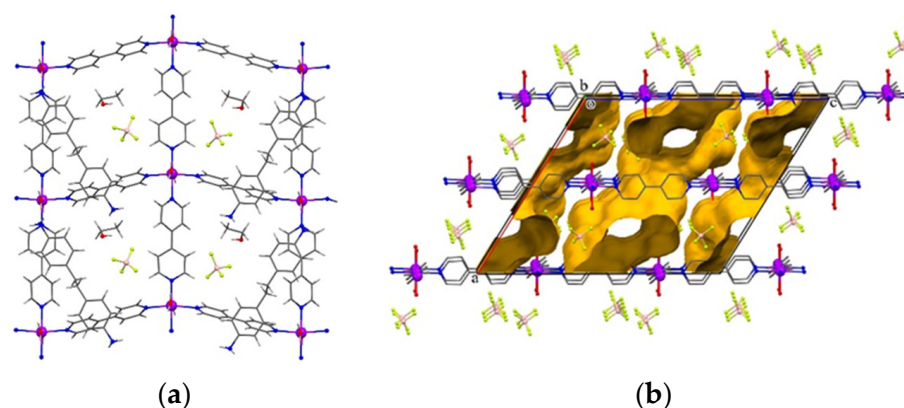


Figure 6. Compound **6**. (a) Fragment of cationic 2D grid with outer-sphere tetrafluoroborate anions and dadpe and EtOH guest molecules. (b) Crystal packing with voids shown in yellow.

Coordination polymer $[\text{Cd}(\text{adi})(\text{dadpe})](\text{H}_2\text{adi})_n$ (**7**) crystallizes in the monoclinic $P2_1/c$ space group and represents a 2D coordination network with **sql** topology (Figure 7a). Each Cd(II) atom takes a distorted octahedral N_2O_4 coordination geometry originating from adipate anions and neutral dadpe-bridging ligands. The same ligands are situated in trans-positions in Cd polyhedron and adi ligand coordinates in a bidentate-chelate bridging mode, while dadpe coordinates in a bidentate-bridging mode. Both coordinated ligands reside on inversion centers, and dadpe undergoes extended trans-conformation identical to that registered in **1**, **5** and **6**, while adi undergoes significantly twisted conformation with resolved disordering of the central methylene fragment. The rhombohedral meshes in the coordination layer have dimensions 10.175×15.102 Å², calculated as Cd...Cd separations across the adi and dadpe-bridging ligands, respectively. The coordination layers are situated parallel to the ac coordination plane (Figure 7b) and accommodate H₂adi molecule as a guest held in the crystal via $\text{NH}\cdots\text{O}$ and $\text{OH}\cdots\text{O}$ hydrogen bonds. Voids, occupied by H₂adi molecules, comprise 328.51 Å³ or 24.7% of the unit cell volume (Figure 7c).

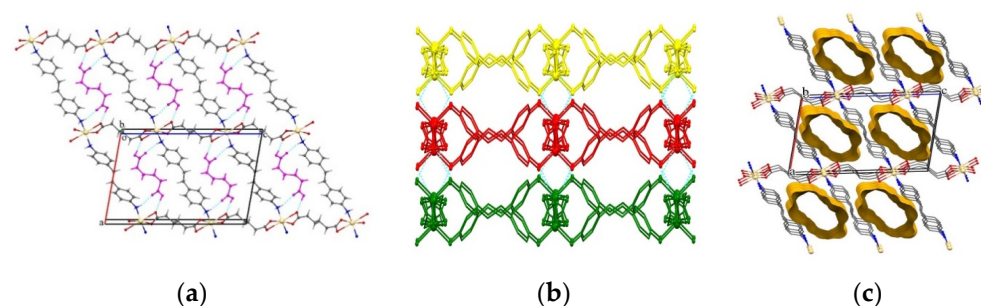


Figure 7. Compound **7**. (a) Fragment of 2D grid with H-bonded H₂adi shown in magenta color. (b) Stacking of coordination layers. (c) Crystal packing with voids shown in yellow.

3.3. Hirshfeld Surface Modeling of Coordination Compounds 1–3, 7

Various studies show that the way coordination compounds pack in the crystals is influenced by intermolecular interactions, and different methods are used to study their types. One of these methods is Hirshfeld surface analysis [32]. The size and shape of Hirshfeld surfaces (HS) help identify intermolecular interactions and classify molecular crystals in terms of packing similarities [33]. The CrystalExplorer program is used to generate Hirshfeld surfaces, and in our case, we used CrystalExplorer 17.5 [34].

We chose to perform the Hirshfeld surface analysis for four coordination compounds which differ in dimensionality, these being discrete mononuclear complexes **1** and **2**, 1D and 2D coordination polymers, **3** and **7**, with dadpe revealing different structural functions, as the neutral guest in **1**, the terminal monodentate ligand with one amino group free from metal coordination in **2**, and a bidentate-bridging ligand in **3** and **7**.

The main contributions to the total HS areas of the molecules **1–3, 7** are depicted by the decomposed d_{norm} surfaces (Figure 8a–d) and by the full (Figure 9) and decomposed fingerprint plots (Figures S8–S11 in Supporting Information file). The eight principal types of interaction are H···H, H···O/O···H, H···C/C···H, H···N/N···H, C···O/O···C, C···N/N···C, C···C and O···O contact. The predominant interactions in all cases are H···H; they appear in the middle of the scattered points in the fingerprint maps, ranging from 34.4% in **1** to 53% in **2**. With significantly less contribution, the next most important interactions are H···O/O···H, which vary from 22.4% in **2** to 36.6% in **3**. The C···C contacts associated with π - π stacking interactions are present in three compounds **1, 2** and **3**, but a more obvious contribution is observed in compound **1**, which on the other hand does not reveal any pronounced hydrogen-bonding interactions (Figure 10).

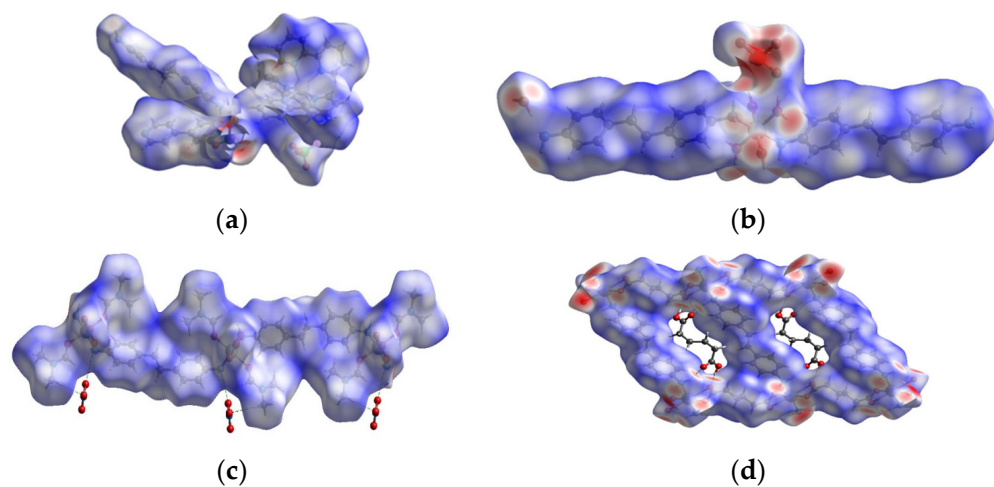


Figure 8. Hirshfeld surfaces mapped with d_{norm} ranging from -0.40 \AA (red) to 2.40 \AA (blue) for crystal structures **1** (a), **2** (b), **3** (c) and **7** (d).

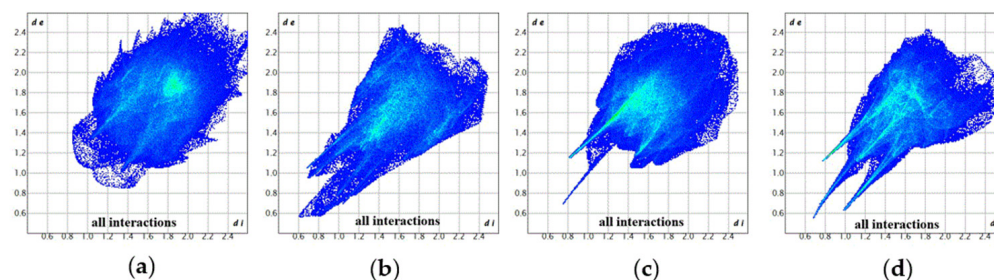


Figure 9. 2D fingerprint plots with d_i and d_e ranging from 1.0 to 2.4 \AA for **1** (a), **2** (b), **3** (c) and **7** (d).

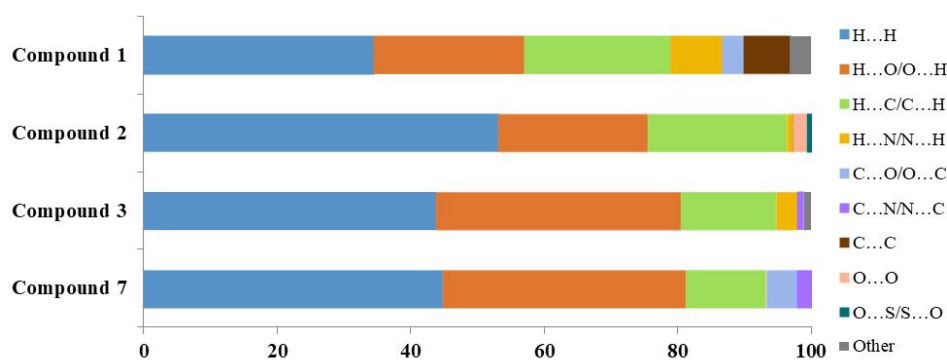


Figure 10. The relative contributions of different types of intermolecular interactions on the basis of Hirshfeld surface analysis of 1–3 and 7.

4. Conclusions

For the first time, Zn/Ni/Co/Cd coordination compounds have been reported and obtained with participation of ditopic flexible ligand, 4,4'-diaminodiphenylethane (dadpe). The dadpe, as a neutral guest, was held in the crystals either via π - π stacking interactions or via $\text{NH}\cdots\text{O}$ hydrogen bonds; meanwhile, as a bidentate-bridging ligand, it gave rise to the 1D coordination polymers or 2D polymeric network used in combination with an adipato ligand. Both coordinated and free amino groups of dadpe participate in hydrogen-bonding systems, thus diversifying the supramolecular architectures. Hirshfeld surface analysis, as a useful tool, helped to evaluate the distribution of intermolecular interactions in the systems with different functions of dadpe ligand.

Supplementary Materials: The following supporting information can be downloaded at: <https://www.mdpi.com/article/10.3390/cryst13020289/s1>, Table S1: Bond lengths and angles for 1–7, Table S2: Hydrogen bonds for 1–7; Figures S1–S7: Infrared spectra for compounds 1–7 and starting ligands; Figures S8–S11: 2D fingerprint plots for distribution of intermolecular contacts in 1–3, 7.

Author Contributions: N.C.—Investigation, data curation, visualization; D.C.—Investigation, data curation, methodology; E.M.—Investigation, data curation, visualization, original manuscript writing; M.S.F.—Conceptualization, Validation, Writing—original draft preparation. All authors have read and agreed to the published version of the manuscript.

Funding: This research was funded by the projects of Agentia Natională pentru Cercetare si Dezvoltare (ANCD) 20.80009.5007.15 and 20.80009.5007.28.

Data Availability Statement: Any additional details are available from the authors.

Conflicts of Interest: The authors declare no conflict of interest.

References

- Noro, S.; Kitaura, R.; Kondo, M.; Kitagawa, S.; Ishii, T.; Matsuzaka, H.; Yamashita, M. Framework engineering by anions and porous functionalities of Cu(II)/4,4'-bpy coordination polymers. *J. Am. Chem. Soc.* **2002**, *124*, 2568–2583. [[CrossRef](#)] [[PubMed](#)]
- McManus, G.; Perry IV, J.J.; Perry, M.; Wagner, B.D.; Zaworotko, M.J. Exciplex Fluorescence as a Diagnostic Probe of Structure in Coordination Polymers of Zn^{2+} and 4,4'-Bipyridine Containing Intercalated Pyrene and Enclathrated Aromatic Solvent Guests. *J. Am. Chem. Soc.* **2007**, *129*, 9094–9101. [[CrossRef](#)] [[PubMed](#)]
- Melnic, E.; Coropceanu, E.B.; Forni, A.; Cariati, E.; Kulikova, O.V.; Siminel, A.V.; Kravtsov, V.C.; Fonari, M. Discrete Complexes and One-Dimensional Coordination Polymers with $[\text{Cu}(\text{II})(2,2'\text{-bpy})]^{2+}$ and $[\text{Cu}(\text{II})(\text{phen})]^{2+}$ Corner Fragments: Insight into Supramolecular Structure and Optical Properties. *Cryst Growth Des.* **2016**, *16*, 6275–6285. [[CrossRef](#)]
- Croitor, L.; Coropceanu, E.B.; Chisca, D.; Baca, S.G.; van Leusen, J.; Kogerler, P.; Boursh, P.; Kravtsov, V.C.; Grabco, D.; Pyrtsac, C.; et al. Effects of Anion and Bipyridyl Bridging Ligand Identity on the Co(II) Coordination Networks. *Cryst. Growth Des.* **2014**, *14*, 3015–3025. [[CrossRef](#)]
- Du, M.; Li, C.-P.; Liu, C.-S.; Fang, S.-M. Design and Construction of Coordination Polymers with Mixed-Ligand Synthetic Strategy. *Coord. Chem. Rev.* **2013**, *257*, 1282–1305. [[CrossRef](#)]

6. Pal, A.; Chand, S.; Senthilkumar, S.; Neogi, S.; Das, M.C. Structural Variation of Transition Metal Coordination Polymers Based on Bent Carboxylate and Flexible Spacer Ligand: Polymorphism, Gas Adsorption and SC-SC Transmetalation. *CrystEngComm* **2016**, *18*, 4323–4335. [[CrossRef](#)]
7. Lozovan, V.; Kravtsov, V.C.; Coropceanu, E.B.; Siminel, N.; Kulikova, O.V.; Costriucova, N.V.; Fonari, M.S. Seven Zn(II) and Cd(II) 1D Coordination Polymers Based on Azine Donor Linkers and Decorated with 2-Thiophenecarboxylate: Syntheses, Structural Parallels, Hirshfeld Surface Analysis, and Spectroscopic and Inclusion Properties. *Polyhedron* **2020**, *188*, 114702. [[CrossRef](#)]
8. Czyłkowska, A.; Pietrzak, A.; Szczesio, M.; Rogalewicz, B.; Wojciechowski, J. Crystal Structures, Hirshfeld Surfaces, and Thermal Study of Isostructural Polymeric Ladders of La(III) and Sm(III) Coordination Compounds with 4,4'-Bipyridine and Dibromoacetates. *Materials* **2020**, *13*, 4274. [[CrossRef](#)]
9. Carlucci, L.; Ciani, G.; Proserpio, D.H.; Porta, F. New metal–organic frameworks and supramolecular arrays assembled with the bent ditopic ligand 4,4-diaminodiphenylmethane. *CrystEngComm* **2006**, *8*, 696–706. [[CrossRef](#)]
10. Luo, J.; Hong, M.; Wang, R.; Cao, R.; Shi, Q.; Weng, J. Self-Assembly of Five Cadmium(II) Coordination Polymers from 4,4'-Diaminodiphenylmethane. *Eur. J. Inorg. Chem.* **2003**, *9*, 1778–1784. [[CrossRef](#)]
11. Chisca, D.; Croitor, L.; Melnic, E.; Petuhov, O.; Kulikova, O.; Fonari, M.S. Six transition metal–organic materials with the ditopic 4,4'-diaminodiphenylmethane ligand: Synthesis, structure characterization and luminescent properties. *Polyhedron* **2020**, *192*, 114844. [[CrossRef](#)]
12. Zhao, D.; Liu, X.-H.; Zhao, Y.; Wang, P.; Liu, Y.; Azam, M.; Al-Resayes, S.I.; Lu, Y.; Sun, W.Y. Luminescent Cd(II)–organic frameworks with chelating NH₂ sites for selective detection of Fe(III) and antibiotics. *J. Mat. Chem. A* **2017**, *5*, 15797–15807. [[CrossRef](#)]
13. Groom, C.R.; Bruno, I.J.; Lightfoot, M.P.; Ward, S.C. The Cambridge Structural Database. *Acta Cryst. B* **2016**, *72*, 171–179. [[CrossRef](#)] [[PubMed](#)]
14. Kokunov, Y.V.; Kovalev, V.V.; Gorbunova, Y.E. Layered Structure of the Silver Coordination Polymer with Nonrigid Aromatic Diamine {Ag[CH₂(C₆H₄NH₂)₂]₂(CH₃C₆H₄NH₂)}NO₃. *Russ. J. Inorg. Chem.* **2007**, *52*, 1877–1882. [[CrossRef](#)]
15. Kokunov, Y.V.; Gorbunova, Y.E.; Kovalev, V.V. Synthesis and Structure of Silver Coordination Polymer with Extended Ditopic Ligand Containing Terminal Amino Groups [Ag(C₂₄H₂₈N₂)_{1.5}]NO₃. *Russ. J. Inorg. Chem.* **2012**, *57*, 953–958. [[CrossRef](#)]
16. Kokunov, Y.V.; Gorbunova, Y.E.; Kovalev, V.V.; Kozyukhin, S.A. Synthesis, Crystal Structure, and Luminescence Properties of the Tetranuclear Complex of Cadmium(II) Acetate with 4,4'-(1,4-Phenylenediisopropylidene)bisaniline. *Russ. J. Inorg. Chem.* **2012**, *57*, 1553–1558. [[CrossRef](#)]
17. Ltaief, H.; Ben Ali, S.; Mahroug, A.; Ferretti, V.; Graça, M.P.F.; Belhouchet, M. A new copper hybrid compound based on 3,3'-diaminodiphenylsulfone as ligand: Growth, crystal structure, spectroscopic analysis, and thermal behavior. *J. Mol. Struct.* **2023**, *1273*, 134334. [[CrossRef](#)]
18. Ltaief, H.; Mahroug, A.; Paoli, P.; Rossi, P.; Belhouchet, M. A new hybrid compound based on mercury and 3,3'-diaminobiphenylsulfone studied by a combined experimental and theoretical approach. *J. Mol. Struct.* **2020**, *1220*, 128760. [[CrossRef](#)]
19. Smirnov, A.N.; Odintsova, O.V.; Starova, G.L.; Solovyeva, E.V. X-ray and vibrational analysis of amino and chloro bibenzyl 4,4'-derivatives supported by quantum chemical calculations. *J. Mol. Struct.* **2020**, *1202*, 127287. [[CrossRef](#)]
20. Giastas, P.; Yannakopoulou, K.; Mavridis, I.M. Molecular structures of the inclusion complexes b-cyclodextrin ± 1,2-bis(4-aminophenyl)ethane and b-cyclodextrin ± 4,4'-diaminobiphenyl; packing of dimeric b-cyclodextrin inclusion complexes. *Acta Cryst.* **2003**, *B59*, 287–299. [[CrossRef](#)]
21. Behera, N.; Duan, J.; Jin, W.; Kitagawa, S. The chemistry and applications of flexible porous coordination polymers. *EnergyChem* **2021**, *3*, 100067. [[CrossRef](#)]
22. Sheldrick, G.M. A short history of SHELX. *Acta Cryst.* **2008**, *A64*, 112–122. [[CrossRef](#)] [[PubMed](#)]
23. Sheldrick, G.M. Crystal structure refinement with SHELXL. *Acta Cryst.* **2015**, *C71*, 3–8. [[CrossRef](#)]
24. Macrae, C.F.; Bruno, I.J.; Chisholm, J.A.; Edgington, P.R.; McCabe, P.; Pidcock, E.; Rodriguez-Monge, L.; Taylor, R.; Streek, J.; Wood, P.A. Mercury CSD 2.0—New features for the visualization and investigation of crystal structures. *J. Appl. Cryst.* **2008**, *41*, 466–470. [[CrossRef](#)]
25. Spek, A.L. Structure validation in chemical crystallography. *Acta Cryst.* **2009**, *D65*, 148–155. [[CrossRef](#)]
26. David, A.; Thornton, D.A. Metal Complexes of Aniline: Infrared and Raman Spectra. *J. Coord. Chem.* **1991**, *24*, 261–289. [[CrossRef](#)]
27. Park, H.M.; Hwang, I.H.; Bae, J.M.; Jo, Y.D.; Kim, C.; Kim, H.-Y.; Kim, Y.; Kim, S.-J. Anion Effects on Crystal Structures of Cd^{II} Complexes Containing 2,2'-Bipyridine: Photoluminescence and Catalytic Reactivity. *Bull. Korean Chem. Soc.* **2012**, *33*, 1517. [[CrossRef](#)]
28. Zhang, W.; Jiang, Z.; Lu, L. Tris(2,2'-bipyridine-kappa²N,N')cadmium(II) bis(perchlorate) hemihydrate. *Acta Crystallogr.* **2009**, *E65*, m7. [[CrossRef](#)]
29. Vaiana, L.; Platas-Iglesias, C.; Esteban-Gomez, D.; Avecilla, F.; de Blas, A.; Rodriguez-Blas, T. Receptor versus Counterion: Capability of N,N'-Bis(2-aminobenzyl)-diazacrowns for Giving Endo- and/or Exocyclic Coordination of Zn^{II}. *Eur. J. Inorg. Chem.* **2007**, *2007*, 1874–1883. [[CrossRef](#)]
30. Kong, X.-J.; Ren, Y.-P.; Zheng, P.-Q.; Long, Y.-X.; Long, L.-S.; Huang, R.-B.; Zheng, L.-S. Construction of Polyoxometalates-Based Coordination Polymers through Direct Incorporation between Polyoxometalates and the Voids in a 2D Network. *Inorg. Chem.* **2006**, *45*, 10702–10711. [[CrossRef](#)]

31. Lu, J.Y.; Fernandez, W.A.; Ge, Z.; Abboud, K.A. A novel two-fold interpenetrating 3D $4^2.8^4$ network self-assembled from a new 1D coordination polymer. *New J. Chem.* **2005**, *29*, 434–438. [[CrossRef](#)]
32. Hirshfeld, F.L. Bonded-atom fragments for describing molecular charge densities. *Theor. Chim. Acta.* **1977**, *44*, 129–138. [[CrossRef](#)]
33. Wolff, S.K.; Grimwood, D.J.; McKinnon, J.J.; Turner, M.J.; Jayatilaka, D.; Spackman, M.A. *Crystal Explorer*; University of Western Australia: Perth, Australia, 2012.
34. Spackman, M.A.; Jayatilaka, D. Hirshfeld Surface Analysis. *CrystEngComm* **2009**, *11*, 19–32. [[CrossRef](#)]

Disclaimer/Publisher's Note: The statements, opinions and data contained in all publications are solely those of the individual author(s) and contributor(s) and not of MDPI and/or the editor(s). MDPI and/or the editor(s) disclaim responsibility for any injury to people or property resulting from any ideas, methods, instructions or products referred to in the content.